J Solid State Electrochem (2010) 14:203–212
DOI 10.1007/s10008-009-0792-7

ORIGINAL PAPER

Electrochemical modification of Bi_2S_3 coatings in a nickel plating electrolyte

Genovaitė Valiulienė · Albina Žielienė · Birutė Šimkūnaitė · Leonas Naruškevičius · Loreta Tamašauskaitė Tamašiūnaitė · Vidas Pakštas · Algis Selskis

Received: 4 September 2008 / Revised: 16 January 2009 / Accepted: 23 January 2009 / Published online: 20 February 2009

Abstract The electrochemical behavior of Bi_2S_3 coatings in Watts nickel plating electrolyte was investigated using the cyclic voltammetry, electrochemical quartz crystal microbalance, X-ray diffraction, and energy dispersive X-ray analysis methods. During the bismuth sulfide coating reduction in Watts background electrolyte in the potential region from −0.4 to −0.6 V, the Bi_2S_3 and Bi(III) oxygen compounds are reduced to metallic Bi, and the decrease in coating mass is related to the transfer of S^{2-} ions from the electrode surface. When the bismuth sulfide coating is reduced in Watts nickel plating electrolyte, the observed increase in coating mass in the potential region −0.1 to −0.4 V is conditioned by Ni^{2+} ions reduction before the bulk deposition of Ni, initiated by Bi_2S_3. In this potential region, the reduction of Bi(III) oxygen compounds can occur. After the treatment of as-deposited bismuth sulfide coating in nickel plating electrolyte at E=−0.3 V, the sheet resistance of the layer decreases from 10^{13} to 500–700 Ω cm. A metal-rich mixed sulfide $Ni_3Bi_2S_2$–parkerite is obtained when as-deposited bismuth sulfide coating is treated in Watts nickel plating electrolyte at a potential close to the equilibrium potential of the Ni/Ni^{2+} system and then annealed at temperatures higher than 120 °C.

Keywords Bi_2S_3 · $Ni_3Bi_2S_2$ · EQCM · CV · XRD · EDX · SEM

G. Valiulienė · A. Žielienė (✉) · B. Šimkūnaitė · L. Naruškevičius · L. Tamašauskaitė Tamašiūnaitė · V. Pakštas · A. Selskis
Institute of Chemistry,
A. Goštauto 9,
LT-01108 Vilnius, Lithuania
e-mail: redox@ktl.mii.lt

Introduction

Metal sulfides are used as a conductive sublayer in the direct electrochemical metallization of dielectric materials. Due to this reason, their reduction is studied in metal plating electrolytes as well as in supporting ones. From the results of these investigations, a conclusion was made that the reduction of metal sulfide to metal is a necessary step to induce metal electrodeposition [1–3]. As seen from the survey of references [1–6], this process is complicated and accompanied by the chemical or electrochemical interaction between the sulfide layer or the impurities in it and metal ions of the electrolyte. When $Cu_{2-x}S$ was reduced in a Ni plating solution, the sulfur which was incorporated in the sulfide coating during the deposition process reduces to sulfide ions prior to the reduction of $Cu_{2-x}S$ and deposition of Ni [2]. In ref. [3] two cathodic peaks in Ni^{2+}-containing and Ni^{2+}-free electrolytes are related to the electrochemical reduction of a mixture of cobalt sulfide compounds with different structures and oxidation states. Contrary to $Cu_{2-x}S$, CoS, or Bi_2S_3 layers, a layer of Co_2S_3 cannot be electroreduced to metallic Co in a Ni^{2+}-free background electrolyte [4]. The Co_2S_3 converts into NiS when it is cathodically polarized at E~−0.2 V (standard hydrogen electrode [SHE]) in Watts nickel plating electrolyte [4, 5]. When the pyrite electrode was polarized in the Co plating solution, the prebulk deposition (PBD) of one or a few monolayers of Co adatoms occurred before the traditional overpotential or bulk deposition of Co. This metal leads to the formation of a highly ohmic metallic contact, while the deposition of Cu provides a significant Schottky barrier. The PBD of Co is induced by the formation of CoS_2 or mixed Co–Fe sulfides [6].

Bismuth sulfide coatings are easily formed and can be used for the direct metallization of dielectrics [7]. In our

previous work [8], the electrochemical behavior of Bi_2S_3 in a Ni plating electrolyte was studied by the cyclic voltammetry (CV) and X-ray photoelectron spectroscopy (XPS) methods. It was determined that the electrochemical interaction between bismuth sulfide and Ni^{2+} ions occurred in the potential region −0.15 to −0.35 V, and during this interaction, nickel penetrates into the coating. The aim of the present study is to investigate this process in more detail using the electrochemical quartz crystal microbalance (EQCM), CV, X-ray diffraction (XRD), and energy dispersive X-ray analysis (EDX) methods.

Experimental

The coatings were deposited on polished glassy carbon (GC) electrodes for CV measurements and on Au electrodes for CV and microgravimetric measurements using the successive ionic layer adsorption and reaction (SILAR) method. At first, the electrode was dipped at ambient temperature for 120 s in a solution (pH 6), containing 0.08 M $Bi(NO_3)_3$ and 1.2 M glycine [7]. Then, after rinsing of the treated surface with deionized water, the electrode was immersed for 60 s into a solution containing 0.1 M Na_2S and rinsed with deionized water. This constitutes one deposition cycle (N) of the bismuth sulfide coating. The whole cycle described was carried out repeatedly for the required number of deposition cycles. In most cases, the Bi_2S_3 layers were formed by two and four cycles for the experiments on the gold and the GC electrodes.

The voltammetric measurements were performed in a standard cell in Watts background containing 1.2 M Na_2SO_4, 0.2 M NaCl, and 0.5 M H_3BO_3 and Watts nickel plating electrolyte containing 1.2 M $NiSO_4$, 0.2 M $NiCl_2$, and 0.5 M H_3BO_3 at 20±1 °C, using a potentiostat PI-50-1, a programmer PR-8, and a potentiometer XY RECORDER A3 (Russia). The potential scan rate was 50 mV s^{-1}.

Simultaneous CV and microgravimetric studies were performed with a Quartz Crystal Microbalance QCM922 (Princeton Applied Research, USA), two digital voltmeters B7-46/1 connected to a PC through the GPIB-USB-B controller cable (National Instruments, USA). A programming potentiostat PI-50-1 and a sweep generator PR-8 (Russia) were used. AT-cut quartz crystals of 6 MHz fundamental frequency (from Intellemetrics, UK) sputtered by gold from both sides were used. Their geometric areas were 0.636 and 0.283 cm^2, respectively. A standard three-electrode configuration was employed with one side of the quartz crystal as a working electrode, an $Ag/AgCl/KCl_{sat}$ electrode as reference, and a Pt wire as a counter electrode. The measured electrode potential, the current, and the frequency were transferred to the PC every 1.0 s. All the cyclic voltammograms and microgravimetric scans were measured at a scan rate of 10 mV s^{-1} and were swept in the cathodic direction from its stationary value.

Both in voltammetric and EQCM measurements on the GC and Au electrode, the electrode potential was measured with respect to an $Ag/AgCl/KCl_{sat}$ reference electrode and is quoted versus a SHE.

Combined gravimetric and coulometric data allow calculating the total number of the electrons involved in the reaction. EQCM measurements are based on Sauerbrey's equation [9] where the measured frequency changes of the quartz crystal are correlated with the mass changes:

$$\Delta f = -2\frac{f_0^2 \Delta m}{S\sqrt{\mu_q \rho_q}} = -K\Delta m \tag{1}$$

where f_0 is the resonant frequency of the quartz crystal, S is the piezoelectrically active area (cm^2), μ_q is the shear modulus of the quartz ($2{,}947\times10^{11}$ g cm^{-1} s^{-2}), and ρ_q its density (2,648 g cm^{-3}) [10]. K includes all the constants of Eq. 1 and, for fundamental resonance frequency of 6 MHz, is equal 128.152×10^6 Hz g^{-1} corresponding to a sensitivity of 12.26 ng $Hz^{-1}cm^{-2}$.

According to Faraday's law, the charge passed during the electrochemical reaction can be expressed as

$$Q = \frac{Fz\Delta m}{M} \tag{2}$$

where F is the Faraday constant (96,500 C mol^{-1}), z is the number of electrons involved in the reaction, Δm is the mass change during the reaction, and M is the molar mass of the corresponding chemical species. By combining Eqs. 1 and 2, it is possible to determine the ratio m/z by plotting the measured frequency change (Δf) as a function of the charge consumed (Q):

$$m/z = \left|\frac{\mathrm{d}\Delta f}{\mathrm{d}\Delta Q}\right|\frac{F}{K}. \tag{3}$$

The detail derivative of this equation is described in [11, 12].

In the present study, the m/z values were calculated from background corrected data, which were obtained by subtracting blank scans from the measured scans. The blank electrolyte used was Watts background electrolyte.

XRD patterns of the bismuth sulfide powder pressed on the Si crystal were recorded using a D8 diffractometer (Bruker AXS, Germany, 2003) with Cu K_α radiation using a Ni/graphite monochromator. A step-scan mode was used in the 2θ range from 10° to 70° with a step length of 0.02° and a counting time of 5 s per step. To obtain the crystalline phase, the powder was heated at 80, 120, 200, and 250 °C for 6 h under vacuum. The sufficient quantity of powder was obtained by mechanically scrubbing the bismuth sulfide coatings deposited on a GC plate by 12–20 cycles.

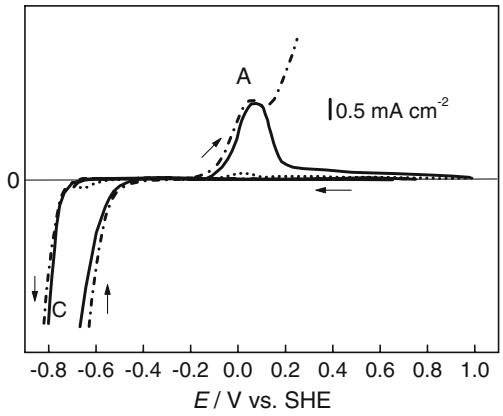

Fig. 1 Cyclic voltammograms recorded in Watts nickel plating electrolyte at pH 4 on GC electrode. Sweep rate 50 mV s^{-1}; 20 °C; potential was swept to −0.69 V (*short dot line*), −0.78 V (*solid line*), −1.0 V (*short dash dot line*)

The chemical composition of the bismuth sulfide coatings was determined by EDX and the surface morphology was examined by scanning electron microscopy (SEM) (EVO-50, Carl Zeiss, 2005).

Results and discussion

The behavior of Bi_2S_3 coatings deposited by the SILAR method on glassy carbon (Bi_2S_3/GC) and Au (Bi_2S_3/Au) electrodes has been investigated in Watts nickel plating electrolyte and in the background solution free from Ni^{2+} ions. In order to thoroughly investigate the nature of electrochemical processes during the reduction of Bi_2S_3 coating in the nickel plating electrolyte when the GC electrode was not coated with a Bi_2S_3 coating, nickel reduction curves were recorded (Fig. 1). The potential was swept in the cathodic direction from the stationary potential value E_s=+0.65 up to −1.0 V (short dash dot line), −0.78 V (solid line), and −0.69 V (short dot line). As seen from Fig. 1, any cathodic peaks do not emerge, while at more negative potentials, cathodic peak C, which results from H_2 and nickel reduction, emerges.

Oxidation peak A of nickel deposited on the GC electrode during the cathodic cycle (in the potential region −0.2 to +0.2 V) is clearly observed when sufficiently negative (−0.78 to −1.0 V) potential values are reached in the cathodic part. When the potential was swept in the cathodic direction of more positive values (up to −0.69 V) and back in the anodic cycle, only small current peak A is observed. After potential sweeping up to −0.5 V, Ni oxidation peak was not seen in the voltammogram. In the literature, most authors relate anodic current peak A with the formation of $Ni(OH)_2$ [13, 14], while others with oxidation of α and β nickel hydrides formed during the cathodic cycle [15]. Sweeping E in the cathodic direction to −1.0 V, then back to the anodic part in the voltammogram, not only current peak A is observed, but a sharp current increase as well, indicating the presence of second anodic peak (are not shown in Fig. 1) of bulk Ni dissolution. The anodic current rising is attributed to bulk Ni dissolution of two different (α and β) NiH_x phases [14].

Figure 2 presents a cyclic voltammogram measured in the background Watts electrolyte [8] sweeping the potential from its stationary value E_s=+0.22 to −1.4 V and back to the anodic part to +1.0 V. The data obtained were discussed in [8] in which it is stated that, in the potential range −0.3 to −0.7 V (cathodic current peak C1), the Bi_2S_3 coating is reduced to metallic Bi and sulfide ions, which move into the bulk of solution:

$$Bi_2S_3 + 6e^- = 2Bi^0 + 3S^{2-}. \quad (4)$$

The current peak A1 that emerged in the anodic cycle at E=+0.72 V should be attributed to the oxidation of metallic Bi formed during the cathodic cycle [16]. The reduction of the formed oxidation products is observed during the second cathodic scan (Fig. 2).

It should be mentioned that the deposited nonreduced Bi_2S_3 coatings contain a reasonable portion of oxygen—up to 45 at.% was detected on the surface and up to 24 at.% in the depth [8]. It seems likely that Bi oxygen compounds can be reduced in the range of cathodic current peak C1 because the equilibrium potential of the reaction:

$$Bi_2O_3 + 6H^+ + 6e^- = 2Bi^0 + 3H_2O \quad (5)$$

is equal to 0.13 V, while its standard potential is 0.37 V.

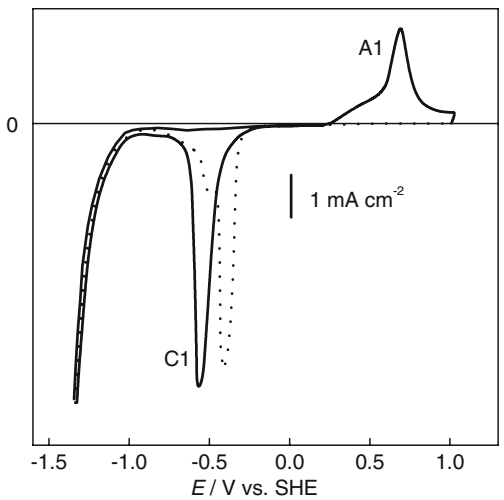

Fig. 2 Cyclic voltammograms of bismuth sulfide coating formed on GC recorded in Watts background electrolyte at pH 4. Sweep rate 50 mV s^{-1}; 20 °C; *dotted line* second scan cycle

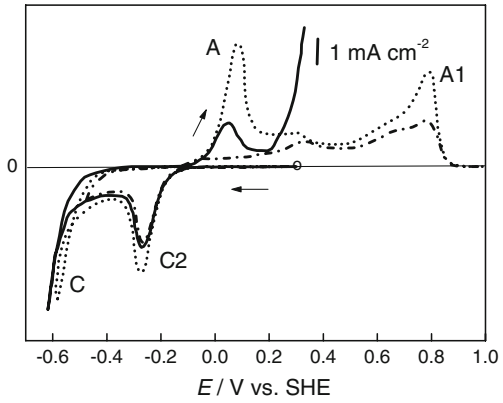

Fig. 3 Cyclic voltammograms of bismuth sulfide coating formed on GC recorded in Watts nickel plating electrolyte at pH 4. Sweep rate 50 mV s^{-1}; 20 °C; potential was swept to −0.48 V (*short dot line*), −0.58 V (*short dash dot line*), −1.0 V (*solid line*)

During reduction of Bi_2S_3/GC coating in the nickel plating electrolyte from E_s=+0.30 to −0.48 V in the cathodic part at E=−0.27 V, current peak C2 is observed in the voltammogram (Fig. 3, short dash dot line). During the reverse potential scan to the anodic part, an increase is observed in the potential range −0.1 to +0.15 V and this can be presumably attributed to the oxidation of nickel reduced in the potential range of peak C2. This increase in anodic current is in the same range as that on GC without Bi_2S_3 coating (Fig. 1, short dot line). A sharper increase in anodic current A1 comprised of two peaks is observed in the potential range +0.15 to +0.9 V.

Inasmuch as in the voltammogram recorded in the nickel plating electrolyte on the glassy carbon sweeping the potential in the cathodic direction to −0.69 V only a slight oxidation peak A of nickel formed during cathodic cycle (Fig. 1, short dot line) and in the potential range +0.5 to +0.9 V no anodic current peaks are observed, it can be supposed that the emerged peak A1 (Fig. 3) is not related with oxidation of nickel, but bismuth compounds because it is observed when Bi_2S_3 coating is reduced in the background Watts electrolyte (Fig. 2). While sweeping the potential in the cathodic direction to −0.58 V (Fig. 3, short dotted line), the values of peaks A and A1 go up markedly. The reason of this is presumably the bulk deposition of Ni when the reduction potential of bismuth sulfide coating was reached. After the potential was swept to the cathodic part up to −1.0 V, a quite substantial quantity of nickel was deposited, and therefore, in the anodic cycle, only oxidation peak A of bulk nickel was observed, whereas peak A1 was covered.

On the basis of the data of reference [8], the reduction of the Bi sulfide coating in the potential range of peak C2 does not occur. Analysis data on the composition of reduced coatings (0.5 h at E=−0.28 V) presented in the same reference show that the coatings contain metallic Ni and NiO. When the curves recorded in the nickel plating electrolyte on the GC (Fig. 1) electrode are compared with those recorded on Bi_2S_3/GC (Fig. 3), it is apparent that, when the electrode is covered with a sulfide coating, the curves are shifted in the direction of more positive potential values; this means a lower cathodic overvoltage and the processes proceed easier.

Because of this, it is supposed that the bismuth sulfide coating present on the GC electrode initiates the adsorption of Ni ions and their reduction (peak C2) at potentials close to the equilibrium potential of the system Ni/Ni^{2+} [17]. The increase in anodic current in the potential range −0.1 to +0.15 V while sweeping the potential to −0.48 V when the potential of nickel bulk discharge is not yet reached (Fig. 3, short dash dot line) is attributed to the oxidation of nickel, deposited in the potential range of cathodic current peak C2. Since, as mentioned above, the deposited coatings contain Bi oxide compounds, reaction 5 is thermodynamically possible in the range of cathodic current peak C2.

Other investigators also observed the peak in almost the same potential region of peak C2 in the CV recorded in nickel plating electrolyte on the other metal sulfides [2, 3, 5, 18]; therefore, its appearance was conditioned by different electrochemical processes. It shows that these processes depend on the nature and composition of the metal sulfide.

According to XPS analysis data of the Bi_2S_3 as-deposited on the GC surface and that after the coating etching with Ar^+ ions for 30 s, elemental sulfur was neither detected on the surface nor at the depth of ~1 nm coating [19]. These assumptions are supported by the data of X-ray energy dispersive analysis of the elemental composition of bismuth sulfide coating. As can be seen from the data in Table 1, the stoichiometric ratio Bi/S does not depend on the coatings thickness and is very close to the theoretical

Table 1 EDX analysis of the elemental composition of Bi_2S_3 coatings deposited on GC

No.	Number of the deposition cycles	at.%		Ratio Bi/S
		Bi	S	
1	4	40.07	59.93	0.69
2	8	39.93	60.07	0.66
3	10	39.95	60.05	0.66
4	15	40.87	59.13	0.67

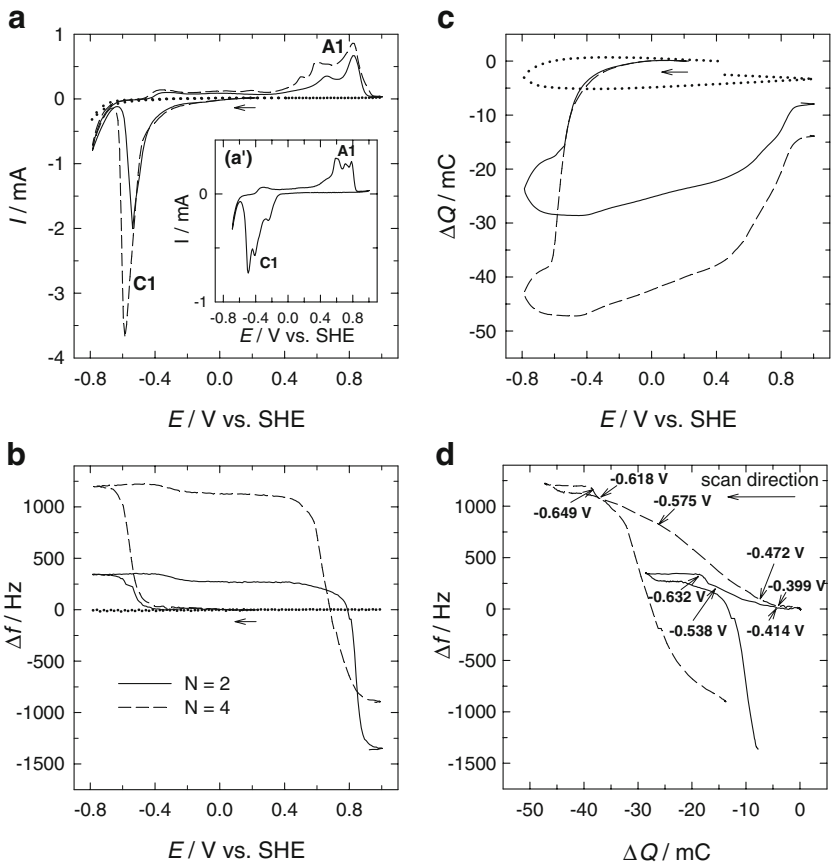

Fig. 4 Cyclic voltammograms for current (**a**), frequency (**b**), charge changes (**c**) and the corresponding Δf versus ΔQ plot (**d**) recorded in Watts background electrolyte at pH 4 on the Bi_2S_3/Au (deposition cycles N=2 and 4, *solid line* and *dashed line*, respectively) and on bare Au electrode (*dotted line*). Sweep rate 10 mV s^{-1}; 20 °C; *inset* second cycle

one—0.66. It can be considered that elemental sulfur is not formed during the deposition of Bi_2S_3 coatings by the SILAR method in contrast to copper sulfide.

The coatings of Bi_2S_3 deposited on Au were investigated by the EQCM method, which gives a possibility to evaluate the mass change of the electrode in the voltammetric experiments and allows describing the electrochemical behavior and the composition of coatings more exactly.

Figure 4a–c represents the cyclic voltammograms for current, frequency, and charge changes, respectively, recorded in Watts background electrolyte at pH 4 for Bi_2S_3/Au with different thicknesses (deposition cycles N=2 and 4) and for a bare Au electrode. In the case of bare Au electrode (Fig. 4a, dotted line), no cathodic current peak and related mass changes (frequency changes) were observed in the CV and the increase in the cathodic current at potentials more negative than −0.6 V is related to hydrogen evolution reaction (Fig. 4a, b). However, during the reduction of Bi_2S_3/Au in Watts background electrolyte, one cathodic current peak is observed at ~−0.58 V (labeled C1). As seen from the data in Fig. 4b, the frequency starts to increase (i.e., the mass starts to decrease) at about the same potential as the current begins to flow (Fig. 4b). It increases until the potential −0.6 V is achieved. Most probably, under the potential region of the cathodic current peak C1 (−0.4 to −0.6 V), the Bi_2S_3 or Bi_2O_3 is reduced to Bi^0, and the decrease in coating mass may be assigned to the detachment of S^{2-} ions from the surface and their transfer into the bulk of the solution. However, the coatings are enriched with oxygen because they were formed by the SILAR method where oxides and hydroxides may appear as a result of the chemical precipitation. Therefore, it may be possible that, during the coating reduction, not only the Bi_2S_3 (reaction 4) but also the Bi(III) oxygen compounds (reaction 5) may be reduced.

The reverse scan shows a broad anodic peak (labeled A1) in the anodic potential region from 0.3 to 0.8 V (Fig. 4a). This anodic peak is associated with the oxidation of bismuth, which was previously reduced during the cathodic scan. As determined from the EQCM data, the anodic current in this potential region is accompanied by a frequency decrease (i.e., mass increase). As seen from the second CV cycle (Fig. 4a′), the shape of the cathodic current peak is similar to that of the anodic current peak. It may be supposed that the cathodic current peak in this case is related to the reduction of Bi oxygen compounds that were previously formed during the anodic scan.

The reduction of the coating depends on its thickness: in the case of a thicker coating (N=4) the cathodic current and frequency as well as charge changes are more pronounced

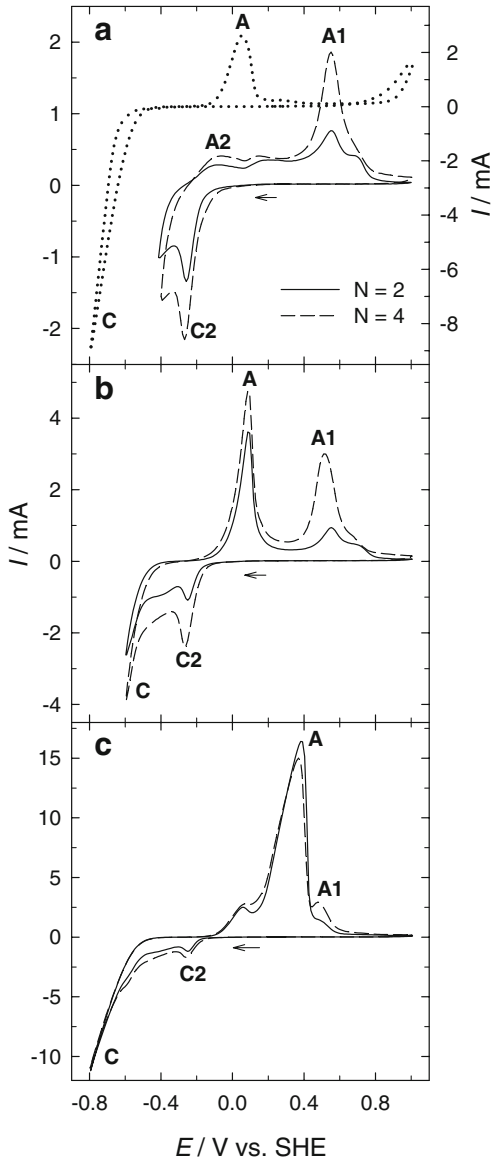

Fig. 5 Cyclic voltammograms for current recorded in Watts nickel plating electrolyte at pH 4 on the Bi_2S_3/Au (deposition cycles N=2 and 4, *solid line* and *dashed line*, respectively) and on bare Au electrode (*dotted line*). Negative potential limit (V): **a** −0.4, **b** −0.6, and **c** −0.8. Sweep rate 10 mV s^{-1}; 20 °C

(Fig. 4). The current of cathodic peak C1 is higher, when the number of the deposition cycles is bigger. The Q consumed in the potential region −0.4 to −0.6 V increases markedly (Fig. 4c, dashed line). The frequency changes are also larger (about fourfold) in the case of a thicker film (Fig. 4b). Whereas during formation of the bismuth sulfide coating other Bi(III) oxygen compounds can be formed and their quantity increases with the number of deposition cycles, it may be predicted that reduction of these compounds conditioned greater charge consumption in the potential range of the cathodic current peak C1.

Figure 4d shows the Δf–ΔQ plot obtained from the data in Fig. 4b, c. As was mentioned, during the coating reduction, reactions 4 and 5 can occur at the same time on the working electrode. The overall reduction process is the sum of these reactions. The calculated theoretical m/z value for reaction 4 is 16 g mol^{-1} and for reaction 5 is 8 g mol^{-1}, so the m/z value of the overall reduction process is 24 g mol^{-1}. The calculated m/z value of −14.04 g mol^{-1} is obtained between the potentials −0.414 and −0.538 V, when the number of the deposition cycles is 2, and −16.16 g mol^{-1} between the potentials −0.399 and −0.472 V, when N=4. These experimental values are close to the Bi_2S_3 reduction, but they are smaller compared to the theoretical value of the overall reduction process. The m/z values obtained at the potential region −0.579 to −0.632 V is −49.91 g mol^{-1}, when N=2. Between the potentials −0.482 and −0.575 V and −0.618 and −0.649 V, the m/z values are −29.89 and −58.3 g mol^{-1}, respectively, when N=4. These values are larger than the theoretical one. It may be due to the greater rate of the electrochemical reduction of Bi_2S_3 and Bi_2O_3 or due to the nonelectrochemical detachment of the coating during the reduction. It may be suggested that a pronounced increase in frequency in the potential region of cathodic peak C1 is conditioned by these processes occurring simultaneously.

According to XPS analysis data [8] of the Bi_2S_3/GC reduced in Watts background electrolyte both on the coating surface and at a depth of 1 nm, a larger amount of oxygen is detected, while the S^{2-} amount detected is considerably lower. It may be concluded that the reaction occurring in the potential region of cathodic peak C1, i.e., the reduction of Bi_2S_3 to Bi^0 is predominant and the decrease in the coating mass is due to the detachment of S^{2-} from the surface.

Figure 5 represents the cyclic voltammograms recorded in Watts nickel plating electrolyte at pH 4 for Bi_2S_3/Au with different thicknesses (N=2 and 4) scanned to different cathodic potential limits. The dotted line shows the CV for a bare Au electrode measured in Watts nickel plating electrolyte (Fig. 5a, dotted line). No cathodic peak was observed in the CV and the increase in the process rate at potentials more negative than −0.7 V (labeled C), indicating the bulk Ni deposition along with H_2 evolution (Fig. 5a, dotted line). The rapid frequency decrease starts at the same potential (Fig. 6a, dotted line). In the reverse scan, the dissolution of Ni begins at about −0.25 V close to the thermodynamic potential for the couple Ni/Ni^{2+}. The anodic current is accompanied by a frequency increase and results in the anodic peak A at 0.1 V. As seen in Figs. 5a and 6a, during the Bi_2S_3/Au reduction in Watts nickel plating electrolyte, one reduction peak C2 at ~−0.28 V is observed, corresponding to a cathodic scan limit of −0.4 V (Fig. 5a). The cathodic current increase and the frequency decrease begins at about −0.1 V and results in the cathodic peak C2, indicating the reduction of Ni^{2+} ions prior to the bulk Ni

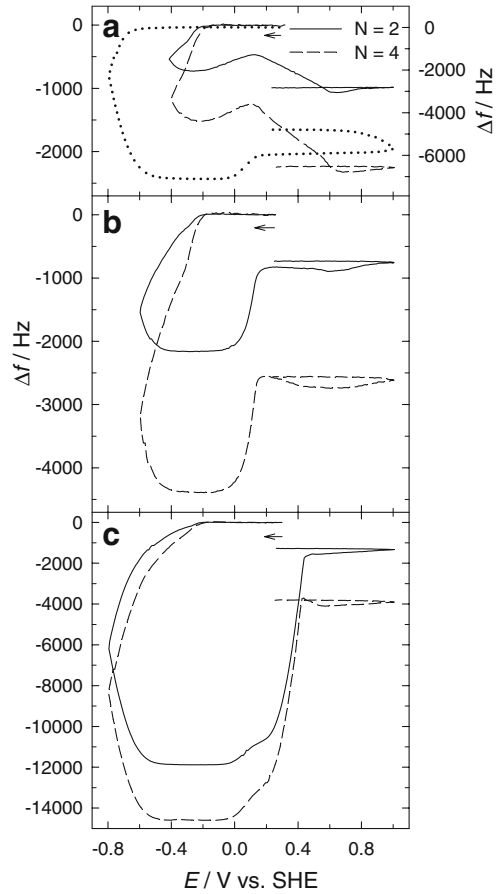

Fig. 6 The frequency change during the scan recorded on the Bi_2S_3/Au (deposition cycles *N*=2 and 4, *solid line* and *dashed line*, respectively) and on bare Au electrode (*dotted line*) in Watts nickel plating electrolyte at pH 4. Negative potential limit (*V*): **a** −0.4, **b** −0.6, and **c** −0.8. Sweep rate 10 mV s^{-1}; 20 °C

deposition. As illustrated in Figs. 5a and 6a, the current and related mass changes are observed at a more positive potential on Bi_2S_3/Au compared to that on the bare Au electrode (Figs. 5a and 6a, dotted line). This result verifies that Bi_2S_3 induces the reduction of Ni^{2+} ions and decreases the Ni overpotential. During the anodic scan, two oxidation peaks are seen: a weaker one A2 at about −0.06 V and a larger A1 at 0.55 V (Fig. 5a). The first anodic peak A2 is under the potential region −0.24 to 0.11 V and is responsible for the dissolution of Ni from the Bi_2S_3/Au surface, as reflected by an increase in anodic current and EQCM frequency. A frequency decrease under the potential region of the second anodic peak A1 (0.12 to 0.8 V) allows to establish the presence of another electrodic process. Similarly, as the anodic current peak A1 occurs in the background electrolyte (Fig. 4a), the presence of an anodic peak at 0.55 V indicates the oxidation of bismuth (Fig. 5). When Bi_2S_3/Au film is reduced both in Watts background and nickel plating electrolyte, the frequency decrease is observed at about the same potential region. So, this anodic peak A1 is attributed to Bi oxidation.

Figure 5b, c shows the CV for Bi_2S_3/Au recorded in Watts nickel plating electrolyte, when the potential is scanned negatively to −0.6 and −0.8 V, respectively. As seen in Fig. 5b, c, in the cathodic scan, C2 is at about the same value, while a stronger one beginning at about −0.4 V (C) verifying the bulk Ni deposition is observed. As indicated by the mass increase (frequency decrease), cathodic peak C, corresponding to a cathodic scan limit of −0.8 V (Fig. 6c) is stronger than that corresponding to a cathodic scan limit of −0.6 V (Fig. 6b). On the reverse scan, anodic peak A at 0.086 and 0.37 V, respectively, correspond to the dissolution of bulk Ni and Ni reduced before the bulk deposition of Ni. When the potential was scanned to more negative values (Fig. 5c), anodic peak A is also remarkably increased. The second anodic peak A1 at 0.5 V is also observed verifying the oxidation of Bi.

Comparing the CV and microgravimetric scans measured on the Bi_2S_3/Au and the bare Au electrode, it is seen that the bulk Ni deposition on the Bi_2S_3/Au (Fig. 5) also occurs

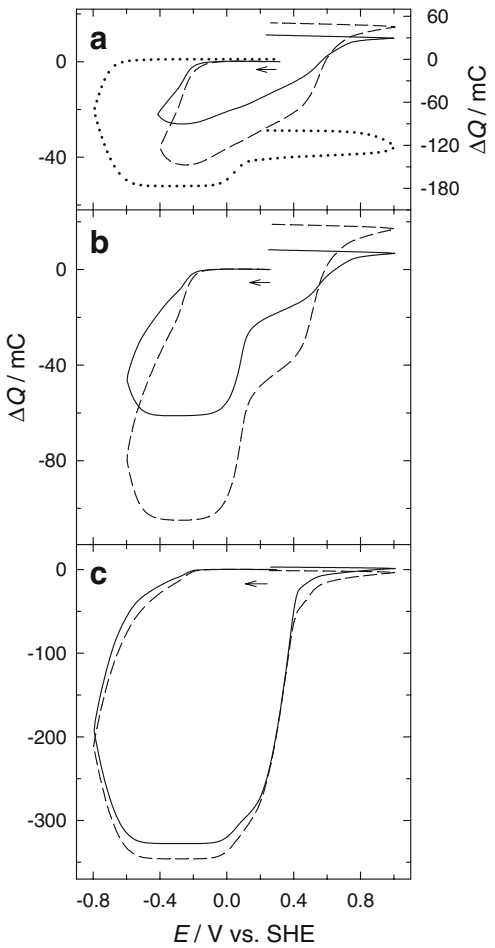

Fig. 7 The charge consumed during the scan recorded on the Bi_2S_3/Au (deposition cycles *N*=2 and 4, *solid line* and *dashed line*, respectively) and on bare Au electrode (*dotted line*) in Watts nickel plating electrolyte at pH 4. Negative potential limit (*V*): **a** −0.4, **b** −0.6, and **c** −0.8. Sweep rate 10 mV s^{-1}; 20 °C

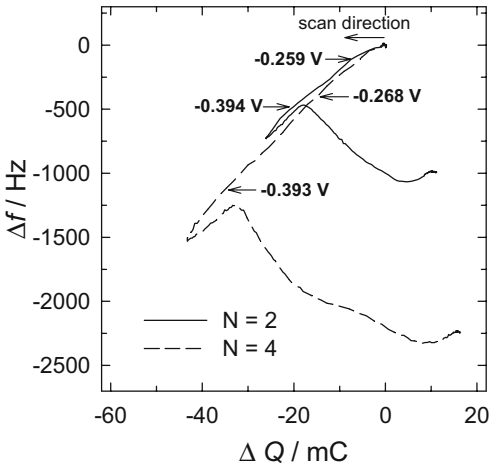

Fig. 8 The Δf–ΔQ plots during the scan recorded in Watts nickel plating electrolyte at pH 4 on the Bi_2S_3/Au (deposition cycles N=2 and 4). Negative potential limit −0.4 V. Sweep rate 10 mV s^{-1}; 20 °C

at more positive potentials than that on bare Au (Fig. 5, dotted line). The bulk deposition of Ni starts at potentials −0.4 and −0.7 V on Bi_2S_3/Au and Au, respectively. As seen in Fig. 6, the related mass changes (Δf) are also observed at a more positive potential on Au coated with bismuth sulfide compared to that on the bare Au electrode.

The Bi_2S_3/Au coating reduction in Watts nickel plating electrolyte depends on the coating thickness. Comparing the corresponding CV and microgravimetric scans measured on Bi_2S_3/Au with different coating thicknesses (N=2 and 4), it is seen that both the current (Fig. 5) and frequency (Fig. 6) as well as charge (Fig. 7) changes are larger when the number of the deposition cycle is 4. The current of cathodic peak C2 is about twofold higher when the number of the deposition cycles increases (Fig. 5, dashed line). Similarly, the Q consumed in the potential region −0.1 to −0.4 V increases pointedly (Fig. 7, dashed line). As seen in Fig. 6 (dashed line), the EQCM frequency changes are about fourfold larger in this potential region. It may be supposed that reduction of these compounds conditions greater current, frequency, and charge changes in the potential region −0.1 to −0.4 V.

Figure 8 shows the Δf–ΔQ plot obtained from the data in Figs. 6a and 7a. During the coating reduction in Watts nickel plating electrolyte, it may be suggested that several reactions can simultaneously occur at the working electrode, i.e., Bi_2O_3 reduction to Bi^0, and reduction of Ni^{2+}:

$$Ni^{2+} + 2e^- \rightarrow Ni^0,\ m/z = 29.35\ \mathrm{g\,mol^{-1}}. \quad (6)$$

As was mentioned, the coating reduction in the background electrolyte occurs at more negative potential values (−0.4 to −0.6 V), so the predominant reaction occurring under the potential region of cathodic peak C2 (−0.1 to −0.4 V) (Fig. 5a) may be attributed to Ni^{2+} ions reduction prior to the bulk deposition of Ni. Due to several processes occurring at the working electrode, the m/z values were calculated from background corrected data, which were obtained by subtracting blank scans from the measured scans under the potential region of cathodic peak C2. The obtained m/z value between the potentials −0.259 and −0.394 V is 27 g mol^{-1} when N=2. The m/z value calculated for a thicker bismuth sulfide coating reduction (N=4) is 31.43 g mol^{-1} (between the potentials −0.268 and −0.393 V). These experimental values are close to the theoretical value of Ni^{2+} ions reduction. The results partly confirm the fact that the mass increase with the cathodic current increase is due to Ni^{2+} ions reduction before the bulk deposition of Ni.

It could be noted that the sheet resistance measurements for a bismuth sulfide layer before and after the treatment differs. The sheet resistance of bismuth sulfide coating deposited on the polyimide surface is ~10^{13} Ω cm and after the reduction in Watts nickel plating electrolyte at a constant potential of −0.3 V (C1 region) for 1 h at pH 4.0 it is 500–700 Ω cm. In this case, the amount of Ni in the treated coating consists 2.32 at.%, as detected by EDX analysis.

Figure 9 shows the powder XRD pattern of the bismuth sulfide coating treated in Watts nickel plating electrolyte at pH 4.0 at a constant potential of −0.28 V. Inasmuch as the deposited coating is amorphous, it was transferred into the crystalline state by annealing for 6 h under vacuum at various temperatures: 80, 120, 200, and 250 °C. The XRD pattern obtained shows that the powder annealed at 80 °C was poor in crystallinity, since no well-resolved peaks were observed except some peaks with small intensity. However, the XRD patterns of the films annealed at 120 °C show

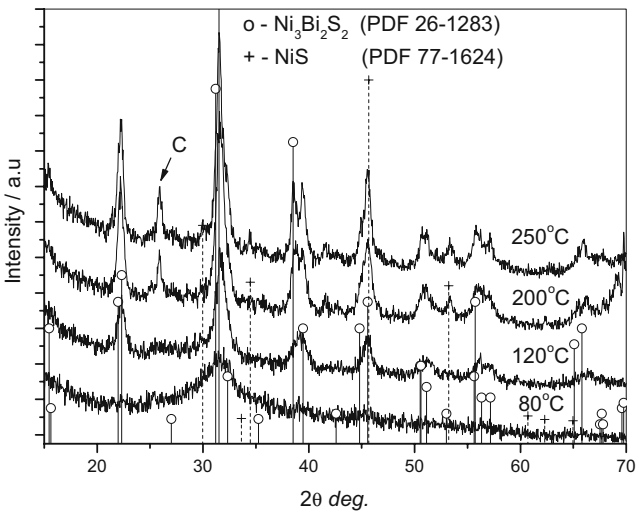

Fig. 9 XRD patterns of Bi_2S_3 coatings deposited on GC plate, treated at E=−0.28 V for 0.5 h in Watts nickel plating solution, scrubbed mechanically, and heated at different temperatures

well-resolved peaks, but not typical of Bi_2S_3 and indicate formation of a new compound $Ni_3Bi_2S_2$ (PDF 26–1283)–parkerite and the improvement of crystallinity up to 10 nm. When annealing the powder at 200 °C, the recrystallization continues and the crystals become larger, but along with the peaks typical of parkerite NiS peaks (PDF 77–1624) are also seen. No essential changes in the diffractogram were observed after annealing of the powder at 250 °C.

The quantitative elemental analysis of the annealed powders was performed for Ni/Bi/S by EDX. It was determined that the elemental composition of the powder annealed at 200 °C is 43.0:24.6:32.4 at.%, which corresponds to the stoichiometric ratio 3.7:2.0:2.7 close to $Ni_3Bi_2S_2$ with a small amount of NiS.

The morphology of the deposits obtained under various conditions was examined by SEM. As seen from the SEM data (Fig. 10a, b), the as-deposited Bi_2S_3 coating and that after treatment in Watts nickel plating electrolyte at a constant potential of −0.28 V for 0.5 h shows overgrowth at certain places. The coatings partially cover the GC surface and aggregates of Bi_2S_3 nanoparticles and separate nanoparticles are observed. When as-deposited Bi_2S_3 film was treated under the same conditions and annealed at 200 °C, the nanoparticles were smaller (Fig. 10c). The fining of nanoparticles could be related with the crystallization, which was confirmed by the XRD data when the peaks of crystalline compounds of $Ni_3Bi_2S_2$ and NiS (Fig. 9) were identified.

According to the XRD results, it can be concluded that a metal-rich mixed sulfide $Ni_3Bi_2S_2$ (parkerite) can be obtained when the bismuth sulfide coating deposited by the SILAR method is treated in Watts nickel plating electrolyte at a potential close to the equilibrium potential of the Ni/Ni^{2+} system and then annealed at temperatures 120–200 °C. It can be used for the creation of a novel method of ternary sulfide coatings formation. Usually, except the minerals parkerite, $Ni_3Bi_2S_2$ is synthesized at high temperature under harsh conditions [20, 21] or at mild conditions [22].

Conclusions

Based on the EQCM data for the frequency, mass, and charge change during the bismuth sulfide coating reduction in Watts background electrolyte, it has been shown that, in the potential region from −0.4 to −0.6 V, the Bi_2S_3 and Bi (III) oxygen compounds are reduced to metallic Bi, and the decrease in coating mass are related to the transfer of S^{2-} ions from the electrode surface.

Reducing the bismuth sulfide coating in Watts nickel plating electrolyte, the observed increase in coating mass in the potential region −0.1 to −0.4 V is conditioned by Ni^{2+} ions reduction, initiated by Bi_2S_3 deposited on the electrode. It is supposed that, in this potential region, the reduction of Bi(III) oxygen compounds occurs.

It has been determined that, after the treatment of as-deposited bismuth sulfide coating in nickel plating electrolyte at E=−0.3 V, the sheet resistance of the layer decreases from 10^{13} to 500–700 Ω cm.

It has been shown that a metal-rich mixed sulfide $Ni_3Bi_2S_2$–parkerite is obtained when as-deposited bismuth sulfide coating is treated in Watts nickel plating electrolyte at a potential close to the equilibrium potential of the Ni/Ni^{2+} system and then annealed at temperatures higher than 120 °C.

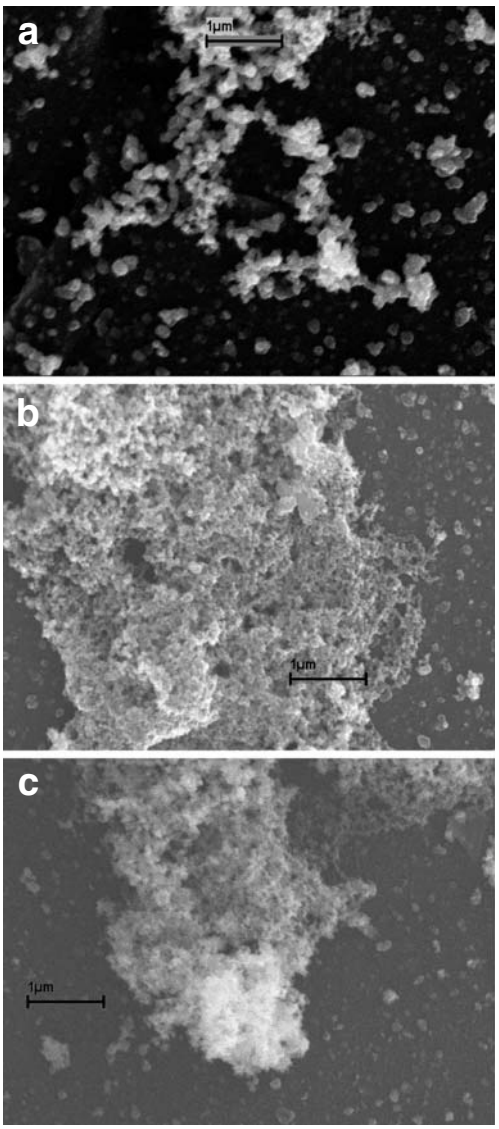

Fig. 10 SEM micrographs of bismuth sulfide coating deposited on GC plate by 10 cycles (**a**), that as **a** treated at E=−0.28 V for 0.5 h in Watts nickel plating solution (**b**), and that as **b** heated at 200 °C under vacuum for 4 h (**c**)

Acknowledgments The authors gratefully acknowledge the support by the Lithuanian State Science and Studies Foundation Grant T-07161.

References

1. Mai TT, Schultze JW, Staikov G (2004) J Solid State Electrochem 8:201 doi:10.1007/s10008-003-0426-4
2. Vinkyavichyus I, Mozhginskene I, Zhelene A, Pilite S (1997) Russ J Appl Chem 70:1900
3. Mai TT, Schultze JW, Staikov G, Muňoz AG (2005) Thin Solid Films 488:321 doi:10.1016/j.tsf.2005.04.069
4. Valiulienė G, Žielienė A, Jasulaitienė V (2005) Chemija 16(2):18
5. Naruškevičius L, Šimkūnaitė B, Valiulienė G, Žielienė A, Jasulaitienė V, Sudavičius A, Baranauskas M, Stankevičius A (2007) Trans IMF 85(4):207
6. Abd El Halim AM, Fiechter S, Tributsch H (2002) Electrochim Acta 47:2615 doi:10.1016/S0013-4686(02)00122-6
7. Baranauskas M (2001) Pat. EP 1174530(A2) EU, Cl. C25D5/54. Method of placing conductor layer on dielectric surface
8. Valiulienė G, Žielienė A, Jasulaitienė V, Naruškevičius L, Pakštas V (2008) Trans IMF 86(6):326
9. Sauerbrey G (1959) Z Phys 155:206 doi:10.1007/BF01337937
10. Buttry D, Ward M (1992) Chem Rev 92:1355 doi:10.1021/cr00014a006
11. Saloniemi H, Kemell M, Ritala M, Leskelä M (2000) J Electroanal Chem 482:139 doi:10.1016/S0022-0728(00)00038-3
12. Kemell M, Saloniemi H, Ritala M, Leskelä M (2000) Electrochim Acta 45:3737 doi:10.1016/S0013-4686(00)00450-3
13. Oblonsky LJ, Devine TM (1995) Corros Sci 37:17 doi:10.1016/0010-938X(94)00102-C
14. Melendres CA, Pankush M (1992) J Electroanal Chem 333(1–2):103 doi:10.1016/0022-0728(92)80384-G
15. Benje M, Eiermann M, Pittermann U, Weil KG (1986) J Phys Chem 90(5):435
16. Grubač Z, Metikoš-Hukovič M (1999) Electrochim Acta 44 (25):4559 doi:10.1016/S0013-4686(99)00174-7
17. Bard AJ (ed) (1975) Encyclopedia of electrochemistry of the elements, vol. 3. Marcel Dekker, New York
18. Valiulienė G, Žielienė A, Jasulaitienė V (2006) Trans IMF 84 (3):162
19. Valyulene G, Zhelene A, Jasulaitene V, Shimkunaite B (2007) Russ J Appl Chem 80:1322 doi:10.1134/S1070427207080113
20. Baranov AI, Olenev AV, Popovkin BA (2001) Russ Chem Bull 50:353
21. Sakamoto T, Wakeshima M, Hinatsu Y (2006) J Phys Condens Matter 18:4417 doi:10.1088/0953-8984/18/17/027
22. Qian G, Shao M, Tong Y, Ni Y (2005) J Cryst Growth 284:412 doi:10.1016/j.jcrysgro.2005.07.013